

SHAPE-TOPOLOGY OPTIMIZATION FOR DESIGNING SHELL STRUCTURES

Hiroataka Nakayama¹, Masatoshi Shimoda²

¹ Graduate School of Toyota Technological Institute
Nagoya, Japan
tontenq.ucd080@gmail.com

² Toyota Technological Institute
Nagoya, Japan
shimoda@toyota-ti.ac.jp

Keywords: Shape, Topology, Optimization, Simultaneous, Shell Structure, SIMP Method, H^1 Gradient Method.

Abstract. *In this study, we propose a new approach for creating the optimal shape and topology of shell structures. By implementing topology optimization in the variable design domain which is optimized by shape optimization at every iteration, the optimal topology and shape is simultaneously determined. The free-form optimization method and the SIMP method for shells are used for shape and topology optimization, respectively. Compliance is minimized under both volume constraints for shape and topology optimization, and out-of-plane shape variation and fictitious density are used as the design variable. The optimum design problem is formulated as a distributed-parameter optimization problem, and the sensitivity functions for shape variation and density are theoretically derived. Both the optimal the optimal shape variation and density distribution are determined by using the H^1 gradient method, where the sensitivity functions are applied under the Robin condition to vary the shape and density. With the proposed method, the compliance is minimized, while maintaining smooth surface and the density distribution. The results show that the proposed simultaneous optimization method provides stiffer and lighter structures with less numerical instabilities.*

1 INTRODUCTION

The researches in the field of shape and topology optimization method has been active in recent years, and successfully applied to optimize structures in many practical automotive or aerospace engineering problems. In the shape optimization problems, the main subject is to find the optimal geometry with the given loading and boundary conditions. In the area of shape optimization for shell structures, the optimization design problem is divided into in-plane and out-of-plane. The former design is used to determine the detail shape or realize weight reduction by changing boundaries. Thus, this boundary shape optimization is usually applied the last stage in design procedure. On the other hand, the latter design has great impact to improve stiffness or some performances by changing surfaces. As the shape of the structure is optimized by varying only the existing boundaries or surfaces of the geometry, it is not able to remove or introduce new boundaries in the design domain. Hence, a general need for optimization methods which is able to allow for a change of the material layout in the design domain.

Topology optimization has been primarily applied to structural problems to obtain lighter structures with optimal material layout. SIMP (Solid Isotropic Material with Penalization) method [1] has been widely used for topology optimization. This approach is to seek density distribution in the design domain, where the elastic tensor of the intermediate density of material is penalized with exponential function of density.

With a conventional topology optimization method for shell structures, it cannot be expected to improve the stiffness because the material layout is determined only in the fixed design domain. On the other hand, shape optimization for shell surface can largely improve the stiffness, but cannot create new holes. Therefore, in this study, we proposed an approach which can create stiffer and lighter shell structures by implemented topology optimization in varying design domain of a shell structure which is optimized by shape optimization.

Some early research for combined shape and topology optimization can be found in papers by Bremicker et al. [2] or Schwarz et al. [3]. Note that the procedure was to find optimal topology first and obtained structure was dealt as the initial design, then boundary shape optimization was additionally applied within obtained design domain in order to increase the performances. Thus the obtained boundaries by topology optimization are modified by shape optimization. Ikeya et al. [4] extended the two-phase optimization method to produce stiffer and lighter shell by carrying out surface shape optimization first and then size optimization. This approach intended to obtain a weight reduced shell with high stiffness by moving shell surface, but the optimization methods are considered separately and it can't take into account the coupling effect of shape and sizing parameters. In other words, these researches are two steps optimization method considering integrated shape and topology or sizing optimization. Ansola et al. [5, 6] and Hassani et al. [7] introduced a simultaneous shape and topology optimization method for shell structures. In their methods, material layout is determined while shape is varying. However, the obtained structures depend on the initial setting of design variables due to the use of parametrization method for shape optimization.

In this study, H^1 gradient method [8-11], a gradient method in a function space, is employed in order to determine the optimal surface for shape optimization and to overcome numerical instabilities for topology optimization while minimizing an objective functional. In our previous work, we developed a free-form optimization method for determining the dynamically natural and optimal shell form. In this work, we apply this method to shape-topology optimization method, and the influence of the method is investigated.

The stiffness maximization problem is solved as a compliance minimization problem under volume constraints for both shape and topology optimization. Shape variation and fictitious

density are optimized by applying the sensitivity functions. The simultaneous optimization problem is solved by means of integrated iterative algorithms, which is simultaneously implemented shape and topology optimization.

2 FORMULATION OF OPTIMIZATION PROBLEM

2.1 Governing equation for a shell structure

As shown in Fig. 1 (a), a shell has an initial design domain Ω , mid-surface A with the boundary of ∂A , side surface S and thickness t . It is assumed for simplicity that a shell structure occupying a bounded domain is a set of infinitesimal flat surfaces. The notations $\{u_{0\alpha}\}_{\alpha=1,2}$, w and $\{\theta_\alpha\}_{\alpha=1,2}$ express the in-plane displacements, out-of-plane displacement and rotational angles of the mid-surface of the shell, respectively in Fig 1 (b). In this paper, the Mindlin-Reissner plate theory is applied concerning plate bending.

The weak form of the state equation with respect to $(\mathbf{u}_0, w, \boldsymbol{\theta}) \in U$ can be expressed as:

$$a((\mathbf{u}_0, w, \boldsymbol{\theta}), (\bar{\mathbf{u}}_0, \bar{w}, \bar{\boldsymbol{\theta}})) = l(\bar{\mathbf{u}}_0, \bar{w}, \bar{\boldsymbol{\theta}}), (\mathbf{u}_0, w, \boldsymbol{\theta}) \in U \quad (1)$$

where the energy bilinear form $a(\cdot, \cdot)$ and the linear form $l(\cdot)$ for the state variables $(\mathbf{u}_0, w, \boldsymbol{\theta})$ are respectively defined as:

$$a((\mathbf{u}_0, w, \boldsymbol{\theta}), (\bar{\mathbf{u}}_0, \bar{w}, \bar{\boldsymbol{\theta}})) = \int_{\Omega} \left\{ C_{\alpha\beta\gamma\delta} (u_{0\alpha, \beta} - x_3 \theta_{\alpha, \beta}) (\bar{u}_{0\gamma, \delta} - x_3 \bar{\theta}_{\gamma, \delta}) + C_{\alpha\beta}^s (w_{, \alpha} - \theta_\alpha) (\bar{w}_{, \alpha} - \bar{\theta}_\alpha) \right\} d\Omega \\ (= \int_A \left\{ c_{\alpha\beta\gamma\delta}^B \kappa_{\gamma\delta} \bar{\kappa}_{\alpha\beta} + c_{\alpha\beta\gamma\delta}^M \epsilon_{0\gamma, \delta} \bar{\epsilon}_{0\alpha, \beta} + k c_{\alpha\beta}^s \gamma_\alpha \bar{\gamma}_\beta \right\} dA) \quad (2)$$

$$l(\bar{\mathbf{u}}_0, \bar{w}, \bar{\boldsymbol{\theta}}) = \int_A (f_\alpha \bar{u}_{0\alpha} - m_\alpha \bar{\theta}_\alpha + q \bar{w}) dA + \int_A t (b_\alpha \bar{u}_{0\alpha} + b_3 \bar{w}) dA + \int_{\partial A} (N_\alpha \bar{u}_{0\alpha} - M_\alpha \bar{\theta}_\alpha + Q \bar{w}) dS \quad (3)$$

It should be noted that U in Eq. (1) is Sobolev space that satisfies the given Dirichlet conditions on each subboundary. In this paper, the subscripts of the Greek letters are expressed as $\alpha = 1, 2$, and the tensor subscript notation uses Einstein's summation convention and a partial differential notation. Loads acting relative to the local coordinate system $(x_1, x_2, 0)$ are defined as: an out-of-plane load q , an in-plane load $\mathbf{f} = \{f_\alpha\}_{\alpha=1,2}$ and an out-of-plane moment $\mathbf{m} = \{m_\alpha\}_{\alpha=1,2}$, an in-plane load $\mathbf{N} = \{N_\alpha\}_{\alpha=1,2}$, a shearing force Q , a bending moment $\mathbf{M} = \{M_\alpha\}_{\alpha=1,2}$ and a body force $\mathbf{hb} = \{hb_i\}_{i=1,2,3}$ are considered as the external forces. In addition, $\{C_{\alpha\beta\gamma\delta}\}_{\alpha, \beta, \gamma, \delta=1,2}$ and $\{C_{\alpha\beta}^s\}_{\alpha, \beta=1,2}$ express an elastic tensor including bending and membrane stresses, and an elastic tensor with respect to the shearing stress, respectively. $\{c_{\alpha\beta\gamma\delta}^B\}_{\alpha, \beta, \gamma, \delta=1,2}$, $\{c_{\alpha\beta}^s\}_{\alpha, \beta=1,2}$ and $\{c_{\alpha\beta\gamma\delta}^M\}_{\alpha, \beta, \gamma, \delta=1,2}$ express orthotropic elastic tensors with respect to bending, shear and membrane component, respectively. The constants k expresses a shear correction factor (assuming $k=5/6$). The notations $\{\kappa_{\alpha\beta}\}_{\alpha, \beta=1,2}$ and $\{\gamma_\alpha\}_{\alpha=1,2}$ express the curvatures and the transverse shear strains.

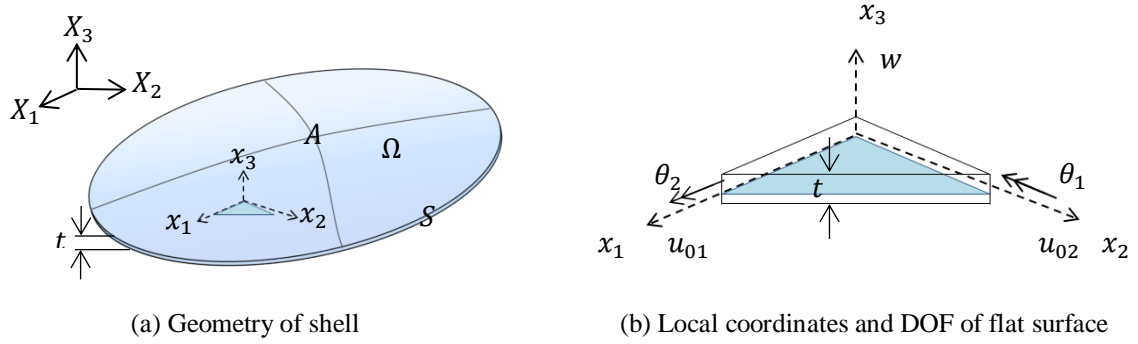


Figure 1: Shell as a set of infinitesimal flat surfaces.

2.2 Compliance minimization problem

In this paper, compliance minimization problem under volume constraints is considered. Letting the volume and the state equations be the constraint conditions, and the compliance be the objective functional to be minimized, a distributed-parameter optimization problem for finding the optimal design velocity field \mathbf{V} and density field ρ can be formulated as:

$$\text{Given} \quad A, \hat{M}_S, \hat{M}_T \quad (4)$$

$$\text{Find} \quad \mathbf{V}, \rho \quad (5)$$

$$\text{Minimized} \quad l(\mathbf{u}_0, w, \theta) \quad (6)$$

$$\text{Subject to} \quad M_S = \int \rho t dA \leq \hat{M}_S, M_T = \int \rho d\Omega \leq \hat{M}_T \text{ and Eq. (1)} \quad (7)$$

where M and \hat{M} denote the volume and its constraint value, respectively.

2.3 Sensitivity analysis

Here, the Lagrange multiplier method is used to transform this constrained shape and topology optimization problem to the non-constrained one. Letting $(\bar{\mathbf{u}}_0, \bar{w}, \bar{\theta})$ and Λ denote the Lagrange multipliers for the state equation and the volume constraints, respectively, the Lagrange functional L associated with this problem can be expressed as:

$$\begin{aligned} L(\Omega, (\mathbf{u}_0, w, \theta), (\bar{\mathbf{u}}_0, \bar{w}, \bar{\theta}), \Lambda) &= l(\mathbf{u}_0, w, \theta) + l(\bar{\mathbf{u}}_0, \bar{w}, \bar{\theta}) - a((\mathbf{u}_0, w, \theta), (\bar{\mathbf{u}}_0, \bar{w}, \bar{\theta})) \\ &\quad + \Lambda(M - \hat{M}_S) + \Lambda(M - \hat{M}_T) \end{aligned} \quad (8)$$

Using the design velocity field \mathbf{V} and density ρ to represent the amount of domain variation, the material derivative \dot{L} of the Lagrange functional L can be expressed as:

$$\begin{aligned} \dot{L} &= l(\mathbf{u}'_0, w', \theta') + l(\bar{\mathbf{u}}'_0, \bar{w}', \bar{\theta}') - a((\mathbf{u}'_0, w', \theta'), (\bar{\mathbf{u}}_0, \bar{w}, \bar{\theta})) - a((\mathbf{u}_0, w, \theta), (\bar{\mathbf{u}}'_0, \bar{w}', \bar{\theta}')) \\ &\quad + \Lambda'(M_S - \hat{M}_S) + \Lambda'(M_T - \hat{M}_T) + \langle \mathbf{Gn}, \mathbf{V} \rangle_s + \langle \mathbf{G}_\rho, \rho \rangle_T, \quad \mathbf{V} \in C_\Theta \end{aligned} \quad (9)$$

$$\langle \mathbf{Gn}, \mathbf{V} \rangle_s = \int_A \mathbf{Gn} \cdot \mathbf{V} dA = \int_A G_A V_n dA + \int_A G_f V_n dA \quad (10)$$

$$\langle \mathbf{G}_\rho, \rho \rangle_T = \int_A G_\rho \delta \rho dA \quad (11)$$

where C_Θ is the suitably smooth function space that satisfies the constraints of the domain variation and notation \mathbf{n} denotes the unit normal vector to the shell surface.

KKT (Karush-Kuhn-Tucker) optimality conditions for this problem are expressed as follows:

$$a((\mathbf{u}_0, w, \theta), (\bar{\mathbf{u}}'_0, \bar{w}', \bar{\theta}')) = l(\bar{\mathbf{u}}'_0, \bar{w}', \bar{\theta}'), \quad (\mathbf{u}_0, w, \theta) \in U, \quad \forall (\bar{\mathbf{u}}'_0, \bar{w}', \bar{\theta}') \in U \quad (12)$$

$$a((\mathbf{u}'_0, w', \theta'), (\bar{\mathbf{u}}_0, \bar{w}, \bar{\theta})) = l(\mathbf{u}'_0, w', \theta'), \quad (\bar{\mathbf{u}}_0, \bar{w}, \bar{\theta}) \in U, \quad \forall (\mathbf{u}'_0, w', \theta') \in U \quad (13)$$

$$\Lambda(M - \hat{M}_s) = 0, \quad \Lambda \geq 0, \quad M - \hat{M}_s \leq 0 \quad (14)$$

By assuming the KKT optimality conditions hold true, the shape and density sensitivity functions G_A and G_ρ for this problem are derived as:

$$G_A = -C_{\alpha\beta\gamma\delta}(u_{0\alpha,\beta} - \frac{t}{2}\theta_{\alpha,\beta})(u_{0\gamma,\delta} - \frac{t}{2}\theta_{\gamma,\delta}) + C_{\alpha\beta\gamma\delta}(u_{0\alpha,\beta} + \frac{t}{2}\theta_{\alpha,\beta})(u_{0\gamma,\delta} + \frac{t}{2}\theta_{\gamma,\delta}) + \Lambda t H \quad (15)$$

$$G_\rho = \frac{\partial c_{\alpha\beta\gamma\delta}^B}{\partial \rho} \theta_{\gamma,\delta} \theta_{\alpha,\beta} + \frac{\partial c_{\alpha\beta\gamma\delta}^M}{\partial \rho} u_{0\gamma,\delta} u_{0\alpha,\beta} + \kappa \frac{\partial c_{\alpha\beta}^S}{\partial \rho} \gamma_\alpha \gamma_\beta + \Lambda \quad (16)$$

where H is twice the mean curvature of mid-area A . In the derivation of G_A and G_f , we assumed that the loading boundaries and surfaces were not varied in the optimization process.

In the SIMP method, the elastic tensor of an intermediate density can be expressed as:

$$C_{\alpha\beta\gamma\delta} = C_{\alpha\beta\gamma\delta}^0 \rho^p \quad (17)$$

where $C_{\alpha\beta\gamma\delta}^0$ is the initial value of the elastic tensor of material and p is the penalization factor.

3 SIMULTANEOUS OPTIMIZATION

In the proposed simultaneous shape and topology optimization method, the optimal design velocity field \mathbf{V} and the optimal density field ρ are determined by using H^1 gradient method. With the proposed method, the update shape and topology of a shell structure is simultaneously implemented without seeing parameter and with smooth surface, while minimizing the objective functional.

3.1 Optimization algorithm

Fig. 2 shows a flowchart of the simultaneous optimization method. At the first step, the equilibrium equation in Eq. (1) is solved using the FEM. In the second step, shape and density sensitivity functions are calculated by Eq. (15) and (16). In the third step, give virtual loading and internal heat generation based on shape and density functions, and then pseudo displacement and temperature field are obtained, respectively. In the fourth step, the equilibrium equation and Poisson's equation are resolved using the virtual loading and internal heat generation, respectively. This third and fourth step is procedure of H^1 gradient method to determine the smooth shell surface and smooth density field. By applying H^1 gradient method, design velocity field \mathbf{V} and density field ρ are updated. After that, this optimization procedure is repeated until the calculated objective function and volumes are converged.

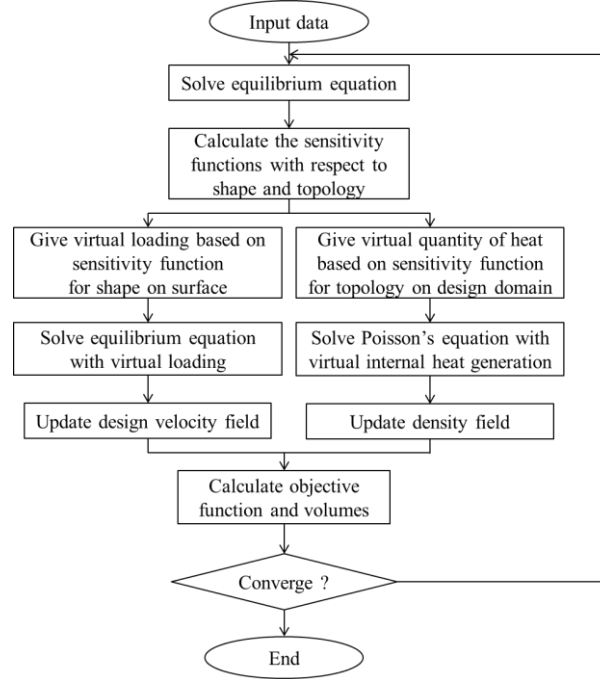


Figure 2: Flowchart of simultaneous optimization method.

3.2 H^1 gradient method for shell structures

The original H^1 gradient method under the Robin condition was introduced by Azegami [8], and Shimoda [10] modified it for free-form shell optimization. To obtain optimal design velocity field \mathbf{V} , the following weak formed governing equation is introduced.

$$a(\mathbf{V}_{0\alpha}, \mathbf{V}_3, \boldsymbol{\theta}), (\bar{\mathbf{u}}_0, \bar{w}, \bar{\boldsymbol{\theta}}) + \alpha \langle (\mathbf{V} \cdot \mathbf{n})\mathbf{n}, (\bar{\mathbf{u}}_0, \bar{w}, \bar{\boldsymbol{\theta}}) \rangle = -\langle \mathbf{G}\mathbf{n}, (\bar{\mathbf{u}}_0, \bar{w}, \bar{\boldsymbol{\theta}}) \rangle, \\ (\mathbf{V}_{0\alpha}, \mathbf{V}_3, \boldsymbol{\theta}) \in C_\Theta, \forall (\bar{\mathbf{u}}_0, \bar{w}, \bar{\boldsymbol{\theta}}) \in C_\Theta \quad (18)$$

where α is distributed spring constant.

In this paper, we apply this method to topology optimization. The concept illustration is shown in Fig. 3. In the SIMP method, it causes the numerical instabilities [12] such as gray scale, checkerboarding pattern and mesh dependency problem because material layout is expressed by density distribution. The proposed H^1 gradient method for topology optimization is also effective to overcome these instabilities.

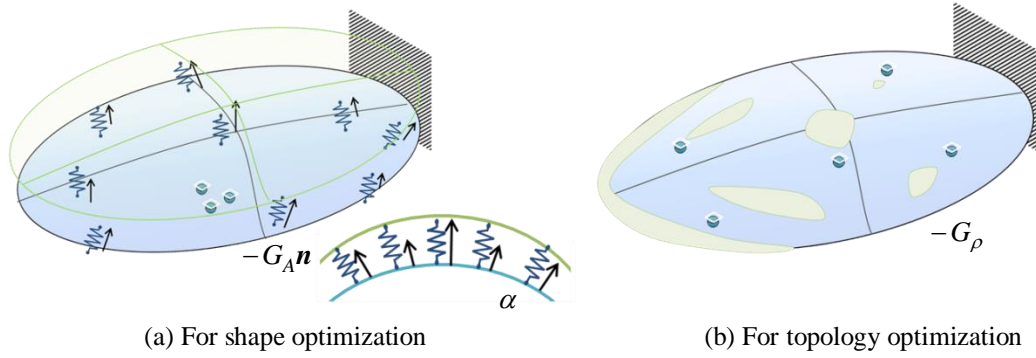
To obtain the optimal density field ρ , the following weak formed Poisson's equation, or the governing equation for ρ is introduced.

$$a(\rho, v) + \varphi_\rho \langle \rho - \rho_0, v \rangle = -\langle G_\rho, \Delta s \rho \rangle, \quad \rho \in C_\rho, \forall v \in C_\rho \quad (19)$$

$$a(\rho, v) = \int_A \rho_{,i} k_{ij} v_{,j} dA \quad (20)$$

where $\Delta s(>0)$ is sufficiently small constant. ρ_0 and C_ρ denote the reference density and the kinematic admissible function space that satisfies Dirichlet condition for density variation, respectively. The notations φ_ρ and k_{ij} are equivalent to the heat transfer coefficient and the thermal conductivity tensor in the steady heat transfer equation, respectively.

In this method, $-G_\rho$ is applied as internal heat generation to the design domain on a pseudo-elastic shell. The density field ρ is calculated as the pseudo-temperature distribution of Poisson's equation and is used to update the original density.

Figure 3: Concept illustrations of H^1 gradient method.

4 NUMERICAL EXAMPLES

In this section, two examples are considered to demonstrate the validity and effectiveness of the simultaneous shape and topology optimization method. In all cases, the material constants are used as the Young's module $E = 210$ GPa, the transverse elasticity module $G = 80.7$ GPa and Poisson ratio $\nu = 0.3$. Furthermore, minimum value of the normalized density is set $\rho_{\min} = 0.01$ to avoid the numerical error.

4.1 Torsion plate problem

Fig. 4 shows the design domain for a square plate. In the stiffness analysis, the plate is supported on three corners and upward force is applied on the other corner in Fig. 4 (a). In the velocity analysis, all edges are simply supported as shown in Fig. 4 (b). The volume constraints of shape and topology are set to 105% and 50% of the initial value, respectively. The material of the shell is modeled using power law SIMP model with a penalty factor of $p = 5$ and the optimization is carried out using 6400 elements with triangle mesh.

Fig. 5 shows the optimal result. As can be seen, a net-shaped topology is created on the X-shaped surface. Fig. 6 shows the iterations history of the compliance and the volumes along with the configurations. Note that the value of compliance is stably reduced by approximately 82% compared with the initial value.

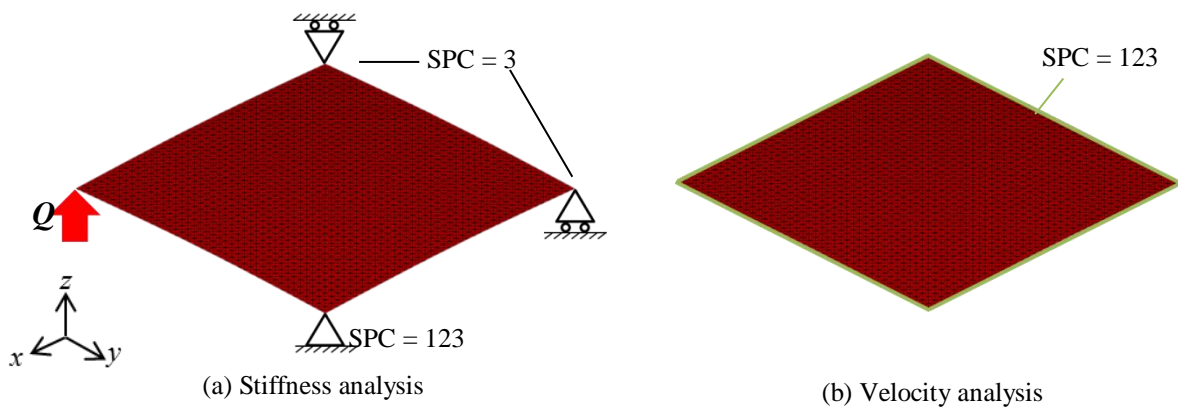


Figure 4: Boundary conditions for a square plate under torsion.

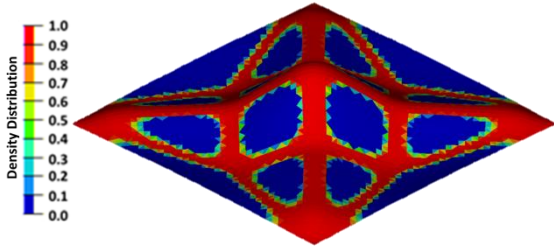


Figure 5: Optimal shape and material layout.

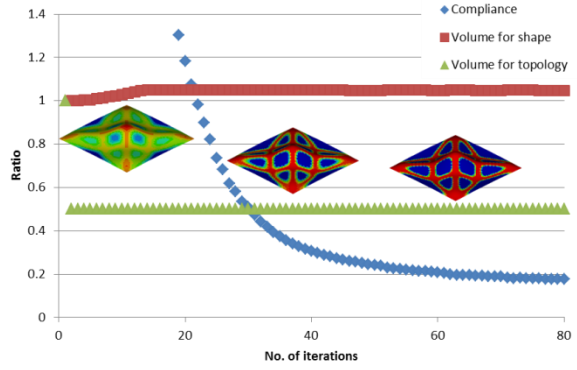


Figure 6: Iterations history of torsion plate.

4.2 Link part problem

The proposed method is applied to a link part model. The initial shape and the problem definition are illustrated in Fig. 7. In the stiffness analyses shown in Fig. 7 (a), the bending moments are applied at the two joints and the other joint is supported. In the velocity analysis shown in Fig. 7 (b), it is assumed that all joints are supported. The volume constraints of shape and topology are set to 100% and 70% of the initial value, respectively. The penalty parameter is set $p = 5$ and the triangle mesh is created by auto-mesh function of HyperMesh [12].

The obtained optimal shape and topology is illustrated in Fig. 8. As it is observed, the constraint area is expanded in the x-direction while the side, bottom and curve area are vertically narrowed, respectively. The material is distributed on the corners and the holes are created on the curve and narrowed area due to reduction the volume. The iterations history is illustrated in Fig. 9. The compliance is gradually decreased by approximately 66% under the constant volume. Hence, the proposed method is successful for finding the optimal shape and material layout.

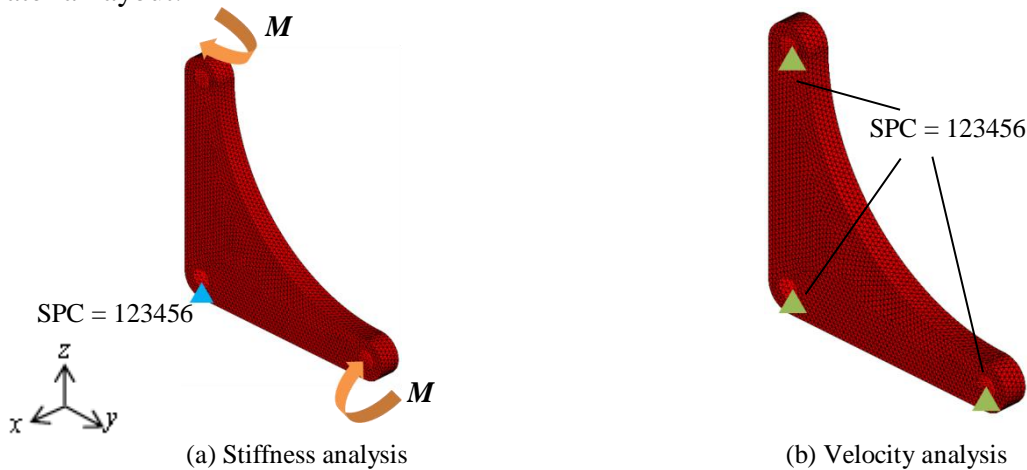


Figure 7: Boundary conditions for link part model under bending moment.

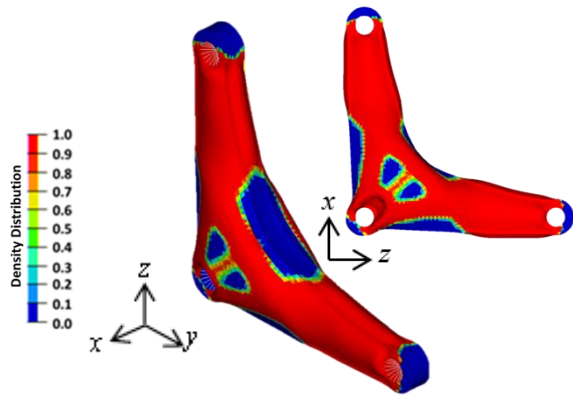


Figure 8: Optimal shape and material layouts

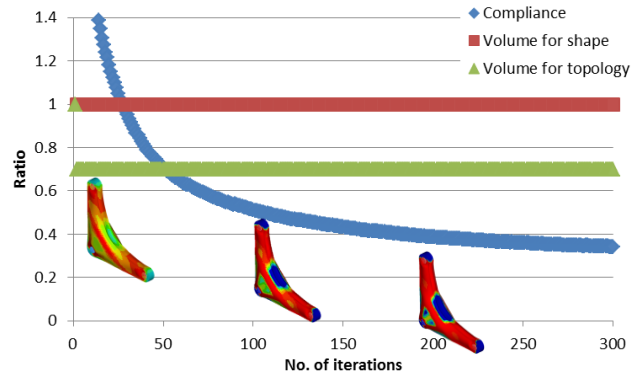


Figure 9: Iterations history of link part model

5 CONCLUSION

This paper described simultaneous shape and topology optimization method for shell structures to minimize the compliance under both shape and topology volume constraints. From a view of stiffness, the conventional topology optimization in a fixed design domain causes the stiffness reduction from the initial solid condition due to the reduction the volume constraint. To overcome this problem, varying design domain is introduced, where the optimal density distribution is determined on varied design domain determined by the shape optimization. The proposed simultaneous optimization method provided lighter and stiffer shell structures where both shape and topology optimization was carrying out concurrently. In the shape optimization problem, the free-form optimization method was applied to vary the shape surface. For the topology optimization problem, the SIMP method was employed to obtain the density distribution. The shape and topology sensitivity functions were derived from governing equation for shell structures and applied to each method. Using H^1 gradient method with sensitivity analysis to optimize shape and material layout, smooth surface was obtained and numerical instabilities for topology were thoroughly solved while reducing the objective functional without shape and topology parameterization.

REFERENCES

- [1] M. Bendsøe, Optimal shape design as a material distribution problem, *Struct. Optim.* 1, 193-202, 1989.
- [2] M. Bremicker, M. Chirehdast, N. Kikuchi and P. Y. Palambros, Integrated topology and shape optimization in structural design, *Mech. Struct. & Mach.*, 19 (4), 551-587, 1991.
- [3] S. Schwarz, K. Maute and E. Ramm, Topology and shape optimization for elastoplastic structural response, *Comput. Methods Appl. Mech. Engrg.* 190, 2135-2155, 2001.
- [4] K. Ikeya, M. Shimoda and J. X. Shi, Multi-objective free-form optimization for shape and thickness of shell structure, *Composite Structures*, 135, 262-275, 2016.
- [5] R. Ansola, J. Canales, J.A. Tarrago and J. Rasmussen, An integrated approach for shape and topology optimization of shell structures, *Computers and Structures*, 80, 449-458, 2002.

- [6] R. Ansola, J. Canales, J.A. Tarrago and J. Rasmussen, Combined shape and reinforcement layout optimization of shell structures, *Struct Multidisc Optim*, 27, 219-227, 2004.
- [7] B. Hassani, M. S. Tavakkoli and H. Ghasemnejad, Simultaneous shape and topology optimization of shell structures, *Struct Multidisc Optim*, 48, 221-233, 2013.
- [8] H. Azegami, A Solution to Domain Optimization Problems, *Trans. of Jpn. Soc. of Mech. Eng.*, 60, 1479-1486, 1994.
- [9] S. Riehl and P. Steinmann, A staggered approach to shape and topology optimization using the traction method and an evolutionary-type advancing front algorithm, *Comput. Methods Appl. Mech. Engrg.*, 287, 1-30, 2015.
- [10] M. Shimoda and Y. Liu, A Non-parametric free-form optimization method for shell Structures, *Structural and Multidisciplinary Optimization*, 50, 409-423, 2014.
- [11] H. Azegami, S. Kaizu and K. Takeuchi, Regular solution to topology optimization problems of continua, *JSIAM Letters*, 3, 1-4, 2011.
- [12] O. Sigmund, Numerical instabilities in topology optimization: A survey on procedures dealing with checkerboards, mesh-dependencies and local minima, *Structural Optimization*, 16, 68-75, 1998.
- [13] <http://www.altairhyperworks.com/product/HyperMesh>